Chem

CellPress

Article

Multicomponent coupling and macrocyclization enabled by Rh(III)-catalyzed dual C–H activation: Macrocyclic oxime inhibitor of influenza H1N1

Biomimetic modularization strategy enables rapid construction of versatile macrocycles with biological activities. A novel Rh(III)-catalyzed dual C–H activation macrocyclization method reported herein allows for the facile access to a diverse array of macrocycles and ultimately facilitates drug discovery.

Hao Wang, Zhongyu Li, Xiangyang Chen, ..., Wei Huang, Kendall N. Houk, Weibo Yang

yangli@simm.ac.cn (L.Y.)
huangwei@simm.ac.cn (W.H.)
houk@chem.ucla.edu (K.N.H.)
yweibo@simm.ac.cn (W.Y.)

Highlights

Rh(III)-catalyzed dual C–H multicomponent coupling and macrocyclization

Biomimetic modularization strategy promotes rapid discovery of lead compounds

Dual C–H macrocyclization is compatible with various reaction coupling

Access to novel macrocyclic oxime inhibitor of influenza H1N1

Wang et al., Chem 9, 1–17
March 9, 2023
https://doi.org/10.1016/j.chempr.2022.10.019

Please cite this article in press as: Wang et al., Multicomponent coupling and macrocyclization enabled by Rh(III)-catalyzed dual C–H activation: Macrocyclic oxime inhibitor of influenza H1N1, Chem (2022), https://doi.org/10.1016/j.chempr.2022.10.019

Chem

CellPress

Article

Multicomponent coupling and macrocyclization enabled by Rh(III)-catalyzed dual C–H activation: Macrocyclic oxime inhibitor of influenza H1N1

Hao Wang,[1,2,7] Zhongyu Li,[1,2,3,7] Xiangyang Chen,[4,7] Jonathan J. Wong,[4,7] Tongyu Bi,[1,2,7] Xiankun Tong,[1,2] Zhongliang Xu,[1,2] Mingyue Zhen,[1,2] Yunhui Wan,[1,2] Li Tang,[1,2] Bo Liu,[1,2,5] Xinlei Zong,[6] Dandan Xu,[1,5] Jianping Zuo,[1,2] Li Yang,[1,2,*] Wei Huang,[1,2,5,*] Kendall N. Houk,[4,*] and Weibo Yang[1,2,5,6,8,*]

SUMMARY

Herein, we describe a practical streamlined two-component dual C–H activation macrocyclization strategy entailing an *in situ*-generated directing group. The reaction mode is based on Rh(III)-catalyzed three-component coupling involving cascade C(sp^3)–H/C(sp^2)–H bond dual activation. The process is facilitated by readily obtainable amidation reagents, namely, aryl-substituted 1,4,2-dioxazol-5-ones, which can be transformed into amide directing groups via a rhodium-nitrene intermediate. DFT calculations revealed that the C–N versus C–C bond formation chemoselectivity was highly controllable. The synthetic utility of this multicomponent reaction is highlighted by the late-stage C–H functionalization of various complex natural macrocyclic compounds, triterpenoids, biologically active molecules, and drugs. Moreover, the developed method enables the expedient and diversified synthesis of complex macrolactams, and phenotypic screening indicated several unique oxime-containing macrolactams accessed via this strategy showing potent anti-Flu (H1N1) activity with no overt cytotoxic effects.

INTRODUCTION

Macrocyclic compounds occupy an important position in medicinal chemistry and supramolecular materials sciences.[1–3] For instance, cyclic peptides have shown a unique capacity for modulating challenging protein-protein interactions, which is challenging to achieve using other small molecules due to relatively shallow protein binding surfaces.[4] Macrocyclic cages have been used in host-guest molecular recognition based on hydrogen bond interactions.[5] The efficient preparation of these macrocyclic molecules via a modular strategy has been of sustained interest. Schreiber et al. proposed a pioneering build/coupling/pair (B/C/P)-based strategy, and Spring et al. used this strategy to generate structurally diverse macrocycle libraries.[6–10] Recently, our group constructed a variety of pseudo-natural macrocycles via an efficient modular biomimetic assembly strategy.[11–14] Notably, macrocyclization reactions and modular strategies have an equally important and crucial role in the synthesis of macrocycles. During the past decades, condensation, alkyne-azide cycloaddition, and ring closing metathesis (RCM) have been the most frequently practiced and important reactions for realizing macrocyclization.[15–18] However, the development of new reactions and strategies for accessing structurally diverse macrocycles remains highly desirable. Ideally, a more

THE BIGGER PICTURE

Although the synthesis of structurally diverse macrocyclic compounds is highly desirable due to their diverse activities, it poses a marked challenge. Arguably, condensation, alkyne-azide cycloaddition, and ring closing metathesis (RCM) are the most frequently practiced reactions for the synthesis of macrocycles. Nonetheless, the development of new reactions and strategies for accessing structurally diverse macrocycles remains highly desirable. Ideally, a straightforward route for the construction of macrocycles would entail multiple C–H activation and two- or multicomponent macrocyclization, which can tolerate several different types of reactions. Such a method would allow for the facile access to a diverse array of macrocycles in a step- and atom-economic way, ultimately facilitating drug discovery.

Please cite this article in press as: Wang et al., Multicomponent coupling and macrocyclization enabled by Rh(III)-catalyzed dual C–H activation: Macrocyclic oxime inhibitor of influenza H1N1, Chem (2022), https://doi.org/10.1016/j.chempr.2022.10.019

straightforward route for the construction of macrocycles would be multiple C–H activation and two- or multicomponent macrocyclization, which can tolerate several different types of reactions.

Fragment-based drug design (FBDD) is an attractive strategy and is widely used in both academia and the pharmaceutical industry to generate drug candidates.[19–22] In particular, natural product (NP)-derived fragments have been frequently utilized due to their diverse structures and biological activities. For example, salicylihalamides and zearalenone bearing a benzannulated scaffold show immunosuppressive activity.[23–25] Roxithromycin tethered with an oxime fragment exhibits antibacterial activity (Figure 1A).[26] Inspired by NP-derived fragments and privileged scaffolds coupled with our interest in constructing macrocycles, we envisaged the construction of benzamide-embedded oxime-substituted macrocycles via a modular strategy. Our retrosynthetic analysis indicated that a two-component dual C–H activation macrocyclization would furnish the target macrocycles using an oxime-substituted precursor and aryl-substituted 1,4,2-dioxazol-5-ones (Figure 1B).

Recently, transition-metal-catalyzed C–H activation intramolecular macrocyclization has emerged as a powerful synthetic tool for forging linear precursors into macrocyclic molecules, benefiting from step and atom economy.[27,28] Significant contributions in this field have been made by the James,[29] Albericio/Lavilla,[30] Chen,[31] Wang,[32] and Ackermann[33] groups, among others, who utilized a pre-installed peptide backbone or heterocycles as directing groups. Inspired by the C–H activation intramolecular macrocyclization reaction mode,[27,28] which originates from a two-component reaction, we concluded that a three-component reaction using editable linkers could be harnessed to achieve dual C–H activation macrocyclization. Additionally, C–H functionalization via three-component reactions represents an ideal synthesis, applicable for the assembly of simple and inexpensive building blocks into structurally diverse molecules of significantly higher value. However, there are three challenging issues to be addressed in this scenario. First, efficient transition-metal-catalyzed two-component dual C–H activation macrocyclization remains elusive due to low reactivity and the tendency for dimerization.[31] If successful, such a protocol would not only provide a practical alternative synthetic macrocyclization route but would also promote further structural diversification of macrocycles. Second, aryl-substituted 1,4,2-dioxazol-5-ones as metal nitrene precursors have been widely studied in metal-catalyzed intermolecular or intramolecular C–H amidations.[34–43] It is noteworthy that the absence of such metal nitrenes in macrocyclization strategies that operate via dual C–H activation is puzzling. Third, although pre-installed or transient reversible directing group strategies have been widely utilized for two-component coupling of inactive C(sp^3)–H,[44–47] the three-component extension thereof remains an unanswered challenge due to the chemoselectivity issue.

Herein, we report the successful realization of these ideas via a new *in situ*-generated directing group strategy, which utilizes a readily obtainable amidation reagent and aryl-substituted 1,4,2-dioxazol-5-ones to form amide groups that efficiently promote Rh(III)-catalyzed two-component dual C–H activation macrocyclization and multicomponent coupling (Figures 1B and 1C).

Results and discussion

To verify the feasibility of two-component dual C–H activation macrocyclization, we first investigated three-component coupling involving inactive C(sp^3)–H bonds using our new *in situ*-generated directing group strategy (Figure 2A). Oxime (**1**), aryl-substituted 1,4,2-dioxazol-5-one (**2**), and alkene (**3**) were applied as the

[1]Chinese Academy of Sciences Key Laboratory of Receptor Research, Shanghai Institute of Materia Medica (SIMM), Chinese Academy of Sciences, Shanghai 201203, China

[2]University of Chinese Academy of Sciences, Beijing 100049, China

[3]Nano Science and Technology Institute, University of Science and Technology of China, Suzhou, Jiangsu 215123, China

[4]Department of Chemistry and Biochemistry, University of California, Los Angeles, CA 90095, USA

[5]School of Pharmaceutical Science and Technology, Hangzhou Institute for Advanced Study, University of Chinese Academy of Sciences, Hangzhou 310024, China

[6]School of Chinese Materia Medica, Nanjing University of Chinese Medicine, Nanjing, Jiangsu 210023, China

[7]These authors contributed equally

[8]Lead contact

*Correspondence: yangli@simm.ac.cn (L.Y.), huangwei@simm.ac.cn (W.H.), houk@chem.ucla.edu (K.N.H.), yweibo@simm.ac.cn (W.Y.)

https://doi.org/10.1016/j.chempr.2022.10.019

Please cite this article in press as: Wang et al., Multicomponent coupling and macrocyclization enabled by Rh(III)-catalyzed dual C–H activation: Macrocyclic oxime inhibitor of influenza H1N1, Chem (2022), https://doi.org/10.1016/j.chempr.2022.10.019

CellPress

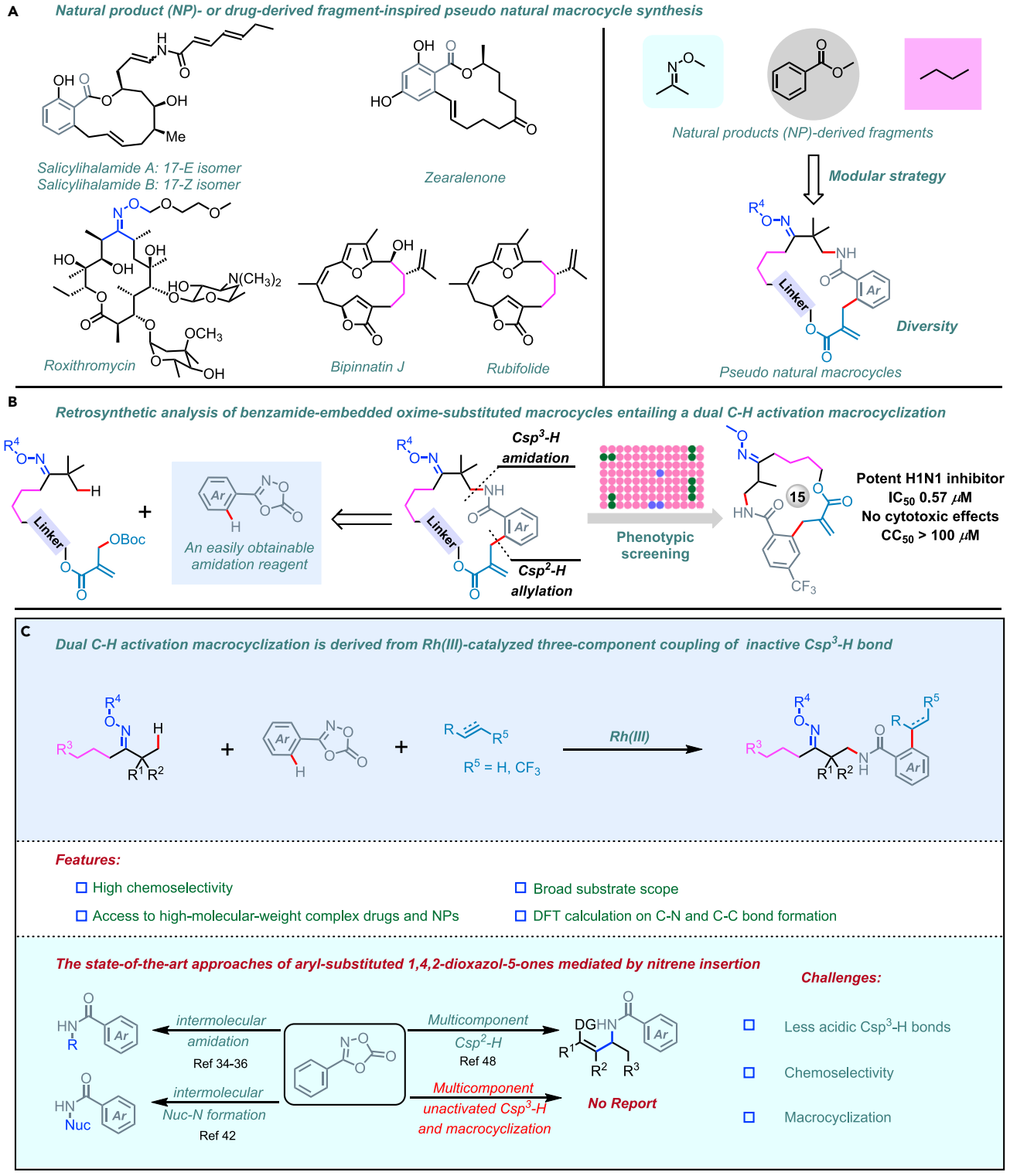

Figure 1. Multicomponent coupling inspired Rh(III)-catalyzed two-component dual C–H activation macrocyclization

(A) Natural product (NP)-derived fragments and their application for the synthesis of pseudo-NP macrocycles via a modular strategy.

(B) Retrosynthetic analysis of benzamide-embedded oxime-substituted macrocycles entailing a two-component dual C–H activation macrocyclization.

(C) This work: Rh (III)-catalyzed three-component coupling of inactive C(sp^3)–H.

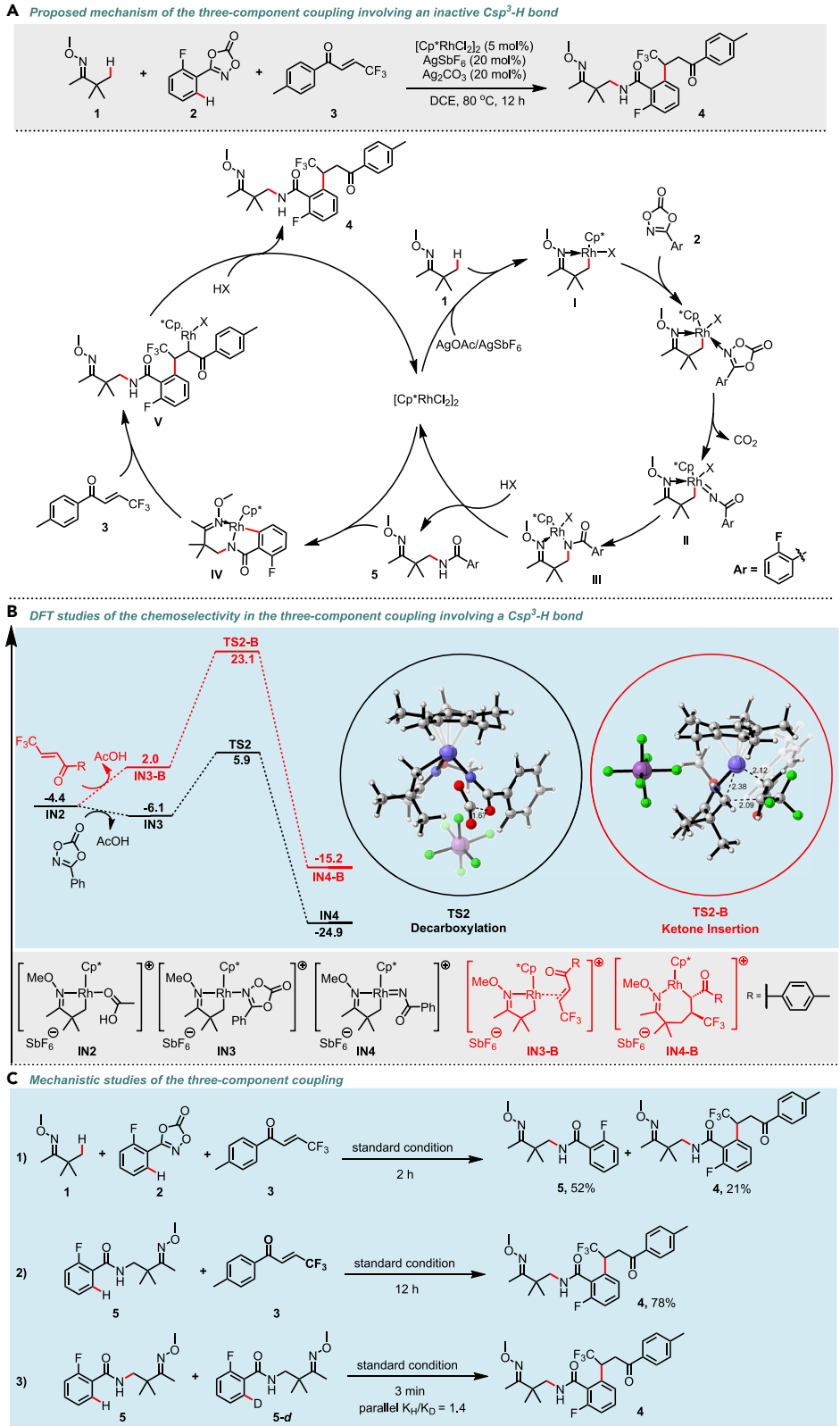
A Proposed mechanism of the three-component coupling involving an inactive Csp3-H bond
[Cp*RhCl2]2 (5 mol%)
AgSbF6 (20 mol%)
Ag2CO3 (20 mol%)
DCE, 80 °C, 12 h
HX
AgOAc/AgSbF6
[Cp*RhCl2]2
CO2
Ar =
B DFT studies of the chemoselectivity in the three-component coupling involving a Csp3-H bond
TS2-B
23.1
TS2
5.9
AcOH
2.0
IN3-B
-4.4
IN2
-6.1
IN3
-15.2
IN4-B
IN4
-24.9
TS2
Decarboxylation
TS2-B
Ketone Insertion
IN2
IN3
IN4
IN3-B
IN4-B
C Mechanistic studies of the three-component coupling
standard condition
2 h
5, 52%
4, 21%
12 h
4, 78%
3 min
parallel KH/KD = 1.4

Figure 2. C–H activation intermolecular macrocyclization originates from three-component reaction

(A) Proposed mechanism of the three-component coupling involving an inactive C(sp^3)–H bond.

(B) DFT studies of the chemoselectivity in the three-component coupling involving a C(sp^3)–H bond.

(C) Mechanistic studies of the three-component coupling.

substrates. As depicted in Figure 2B, the process commences with anti-anion exchange to form the active catalytic species, which then induces C(sp^3)–H bond activation of oxime (**1**) to generate 5-membered ring metal complex **I**. Next, aryl-substituted 1,4,2-dioxazol-5-one (**2**) coordinates to the metal center of **I** and produces cyclic nitrene intermediate **II** upon release of CO_2, followed by migratory insertion to afford amidation intermediate **III** or amidation intermediate product **5**.[34] Subsequently, the catalytic species could continuously induce C(sp^2)–H bond activation of **5** assisted by the *in situ*-generated amide directing group to form fused 5–6-membered ring intermediate **IV**. Intermediate **IV** is expected to react with various alkenes (**3**), followed by protodemetallation, β-O elimination or β-H elimination. Ultimately, structurally diverse products were constructed via appropriate alkylation, allylation, and olefination (Figure 3 in the main text). Very recently, the Ellman and Glorius groups have demonstrated the power of Rh(III) catalysis in elegant three-component C(sp^2)–H bond cascade reactions.[48,49] Inspired by these works, through extensive reaction condition optimization (see Tables S1–S4 for more details), it was identified that $[Cp^*RhCl_2]_2/AgSbF_6$ was the optimal catalyst and proved to be compatible with a number of synthetically useful cascade C–H functionalizations, including C–H alkylation, allylation, and olefination. It should be noted that the order of the C–N/C–C bond formations of these cascade reactions is distinct from that in Ellman's work, wherein they described an intriguing Cp*Rh(III)-catalyzed three-component C(sp^2)–H bond cascade C–C/C–N reaction. We surmised that the choice of C–H substrates herein, instead of alkenes, was the major reason for the distinct reaction order. The C(sp^2)–H bond in the substrates reacted more readily with alkenes via alkene insertion than the C(sp^3)–H bond. We also conducted control experiments. The reaction between the oxime and α, β-unsaturated ketone did not provide any products, but the reaction between the oxime and dioxazolone readily generated the C–H activation amidation product. The excellent chemoselectivity and distinctive pathway were further evidenced by DFT calculations at the M06/SDD (Rh, Ag, Sb), 6-311++G(d, p), SMD (DCE)//B3LYP-D3/LANL2DZ(Rh, Ag, Sb), and 6-31G(d) level of theory. The computational details and full free energy profiles are shown in the supplemental information. Dissociation of the Rh precatalyst dimer and coordination of both the acetate and oxime substrate results in the formation of reactant complex **IN1** with an exothermic energy change of 4.3 kcal/mol (Figure S7). The concerted metalation deprotonation (CMD) process is reversible with a free energy of 12.6 kcal/mol and forms **IN2**. As shown in Figure 2C, the coordination of the dioxazolone and extrusion of acetic acid generates **IN3**. The subsequent formation of nitrene intermediate **IN4** occurs via CO_2 release through **TS2** with a low free energy of 5.9 kcal/mol. Migratory insertion of the α, β-unsaturated ketone through **TS2-B** is less favorable with a much higher free energy of 23.1 kcal/mol. This may be because the dioxazolone coordinates much more strongly to the metal center than the ketone. The ensuing nitrene insertion to form the amidation intermediate **IN5** through **TS3** occurs readily with a free energy barrier of 10.5 kcal/mol. Then, C(sp^2)–H bond activation proceeds via **TS4** with a free energy barrier of 13.1 kcal/mol to form fused 5–6-membered ring intermediate **IN7** (Figure S8). Subsequent alkene insertion via **TS5** is the rate-determining step with a total free energy barrier of 28.7 kcal/mol. Finally, the product is formed through protodemetallation aided by an external acetic acid through **TS6**. β-Hydride elimination via **TS6-B** results in a positive charge on the exceptionally electron-deficient α-carbon, resulting in

Please cite this article in press as: Wang et al., Multicomponent coupling and macrocyclization enabled by Rh(III)-catalyzed dual C–H activation: Macrocyclic oxime inhibitor of influenza H1N1, Chem (2022), https://doi.org/10.1016/j.chempr.2022.10.019

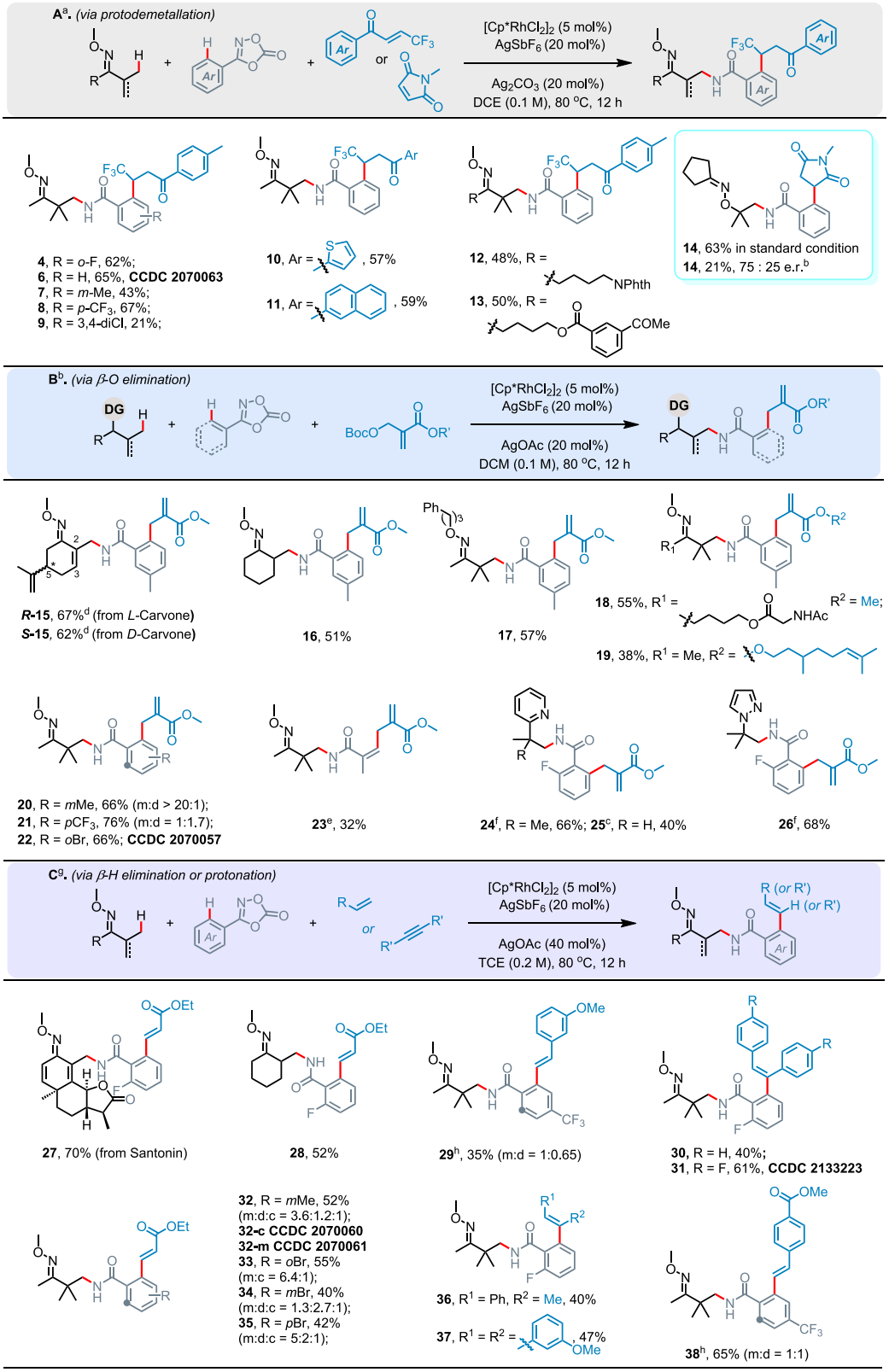

Figure 3. Three-component coupling enabled by Rh(III)-catalyzed dual C–H activation

Yields are based on a 0.1 mmol scale reaction after silica gel chromatography. m, mono; d, di; c, cyclized. [a]Oxime (0.2 mmol, 2.0 equiv), dioxazolone (0.1 mmol, 1.0 equiv), and alkylation reagent (0.15 mmol, 1.5 equiv). [b]Chiral Rh(III) catalyst was used instead of $[Cp^*RhCl_2]_2$, the condition was shown in supporting information. [c]Oxime (0.2 mmol, 2.0 equiv), dioxazolone (0.1 mmol, 1.0 equiv), and allylation reagent (0.15 mmol, 1.5 equiv). [d]Performed with Cs_2CO_3 (20 mol %) instead of AgOAc. [e]AgF (40 mol %) was used instead of AgOAc. [f]Heterocycle (0.15 mmol, 1.5 equiv), dioxazolone (0.1 mmol, 1.0 equiv), allylation reagent (0.2 mmol, 2.0 equiv), and AgOAc (10 mol %). [g]Oxime (0.2 mmol, 2.0 equiv), dioxazolone (0.1 mmol, 1.0 equiv), alkenylation reagent (0.15 mmol, 1.5 equiv). [h]Oxime (0.15 mmol, 1.5 equiv), dioxazolone (0.1 mmol, 1.0 equiv), olefin (0.2 mmol, 2.0 equiv), $[Cp^ERhCl_2]_2$ (5 mol %), $AgSbF_6$ (20 mol %) and $Cu(OAc)_2$ (20 mol %), and DCE/HFIP = 4/1 (1.0 mL), 100°C, air, 12 h. DCE: dichloroethane, DCM: dichloromethane, HFIP: hexafluoroisopropanol.

3.9 kcal/mol higher energy than that of the protodemetallation pathway. Interestingly, intermediate **5** was detected by LC-MS and isolated in 52% yield after 2 h (Figure 2C-1). To further prove that intermediate **5** could be transformed into **4** via C(sp^2)–H bond alkylation, we first synthesized **5** in a yield of 65%, then reacted it with **3** under standard conditions to give the final product **4** in 78% yield (yield over two steps was 51% versus one-pot yield 62%) (Figure 2C-2). Additionally, a parallel kinetic experiment using **5** and its isotopically labeled derivative **5-*d*** provided a kinetic isotope effect (KIE) of $k_H/k_D = 1.4$ (Figure 2C-3). This result indicated that C–H activation may not be the rate-determining step, which is consistent with the DFT calculations.

With the optimized conditions in hand, we first assessed the ketoxime scope of the three-component coupling involving inactive and active C(sp^3)–H bonds. As shown in Figure 3, a range of ketoximes bearing a variety of substituents were found to be suitable substrates in the cascade C–H amidation/alkylation (**4** and **6** to **14**), allylation (**15** to **26**), and olefination (**27** to **38**) reactions. However, acyclic ketoximes containing an α-hydrogen atom reacted sluggishly and gave lower yields because of the presumably more flexible nature of the acyclic conformers. Therefore, we were pleased to find that cyclic ketoximes containing an α-hydrogen atom reacted smoothly to form **16** and **28** in good yield, reinforcing the conformation effect. Furthermore, ketoxime derivatives prepared from the natural perfume (*D*)-carvone, (*L*)-carvone, and santonin, a versatile pesticide, all reacted smoothly to afford the desired products in high yields (**15** and **27**). Furthermore, the use of a chiral Rh catalyst (see supplemental information) facilitated an enantioselective reaction, and enantioenriched maleimide product **14** was obtained in moderate yield and *e.r.*

Although the cascade C–H amidation/alkylation process was slightly hampered in the case of *ortho* bromo-substituted 1,4,2-dioxazol-5-ones, these substrates underwent efficient cascade C–H amidation/olefination or allylation and provided the desired products in 55% and 66% yield (**22** and **33**), respectively. It is worth mentioning that a mixture of mono- or di-olefination (**32**, **34**, and **35**) and mono- or di-allylation products (**21**) was observed in the case of *meta*-or *para*-substituted 1,4,2-dioxazol-5-ones. Interestingly, when the *ortho*-Br, *meta*-Me, or -Br, *para*-Br substituted 1,4,2-dioxazol-5-ones were subjected to the standard cascade C–H amidation/olefination conditions, an unexpected cascade cyclization product was formed along with the desired products (**32–35**).

Furthermore, we assessed the alkene and alkyne scope, and the optimized reactions proved general for various electronically and sterically differentiated α, β-unsaturated ketones, acrylates, styrenes (**29** and **38**), and alkynes (**30** and **31**). For example, CF_3-substituted α, β-unsaturated ketones underwent the cascade C–H amidation/alkylation process smoothly, affording a previously inaccessible class of novel CF_3-substituted amides, which may also have interesting biological properties.[14,50] Importantly, various native heterocyclic directing groups, such as

Please cite this article in press as: Wang et al., Multicomponent coupling and macrocyclization enabled by Rh(III)-catalyzed dual C–H activation: Macrocyclic oxime inhibitor of influenza H1N1, Chem (2022), https://doi.org/10.1016/j.chempr.2022.10.019

pyrazole (**26**) and pyridine (**24** and **25**), were compatible with the multicomponent C(sp^3)–H coupling protocol, and the amidation reagent is not limited to aryl-substituted groups, being extended to alkenyl substituted 1,4,2-dioxazol-5-ones (**23**).

Having successfully developed an efficient three-component coupling method involving an inactive C(sp^3)–H bond, we sought to apply it to the late-stage modification of readily available natural products[51] and two-component dual C–H activation macrocyclization. Alpha-methyl ketone or beta-methyl alcohol are commonly occurring structural motifs in various complex natural macrocyclic compounds, triterpenoids, biologically active molecules and drugs. Although conventionally, these frameworks have been modified via semi-synthesis, this approach is inherently limited because typically only a few positions or active sites can be modified effectively, which curtails the exploration of their structure-activity relationship (SAR). For example, a general and effective method for the selective modification of the challenging β-C(sp^3)–H position of the ketone in the aforementioned sophisticated molecules has not been developed. As shown in Figure 4, the present Rh-catalyzed multicomponent cascade reaction allowed for the streamlined incorporation of an α, β-unsaturated ester into several structurally complex natural products and drugs, including Baccatin III, Moxidectin, Eprinomectin, Milbemycin oxime, and Betulinic acid. The 2015 Nobel Prize in physiology or medicine was awarded for the novel therapy against infections caused by roundworm parasites using avermectins. Notably, a series of avermectin analogs are accessible via the developed coupling protocol.

Subsequently, we returned to the original question of whether this *in situ*-generated directing group strategy could be used to generate benzamide-embedded oxime-substituted macrocycles via two-component dual C–H activation macrocyclization. As illustrated in Figure 5, this strategy demonstrated remarkable tolerance for two-component macrocyclization via C–H amidation/alkylation, allylation, and olefination. Moreover, two-component macrocyclization reactions using ketoximes tethered with different linkers, such as sterically bulky t-butyl, aliphatic ester (**63** to **76**), heteroaryl (**60**), and ether (**48** to **62**), all proceeded smoothly, providing the corresponding 15- to 24-membered macrolactams in synthetically useful yields. The relative configuration of **48** was unambiguously assigned employing X-ray crystal structure analysis. Gratifyingly, the reaction was also compatible with a biaryl moiety (**59**), which is commonly encountered in natural macrocycles that display unique biological properties.[52] To our delight, a ketoxime containing an α-hydrogen atom also proved to be a suitable coupling partner and its successful conversion to macrocyclic products considerably expands the scope of the C–H activation intermolecular macrocyclization method. Next, we evaluated the scope of the aryl-substituted 1,4,2-dioxazol-5-ones in three different types of macrocyclization reactions. Aryl groups with electron-donating and withdrawing substituents at the *ortho*-, *meta*-, and *para*-positions were efficiently accommodated to yield cascade C–H activation macrocyclization products in moderate yields. The allylation protocol was also applicable to bromo-substituted substrate (**67**), which can serve as a useful synthetic handle for various cross-couplings. Additionally, naphthyl-substituted 1,4,2-dioxazol-5-one also underwent C–H amidation/alkylation and allylation/macrocyclization smoothly, affording the corresponding products in 47%, and 36% isolated yield (**56** and **71**), respectively.

Interestingly, the orientation of the double bond could be controlled by choosing suitable alkene coupling partners. *Exo*-alkene products were obtainable via Rh-catalyzed C–H amidation/allylation macrocyclization, whereas endo-alkene

Please cite this article in press as: Wang et al., Multicomponent coupling and macrocyclization enabled by Rh(III)-catalyzed dual C–H activation: Macrocyclic oxime inhibitor of influenza H1N1, Chem (2022), https://doi.org/10.1016/j.chempr.2022.10.019

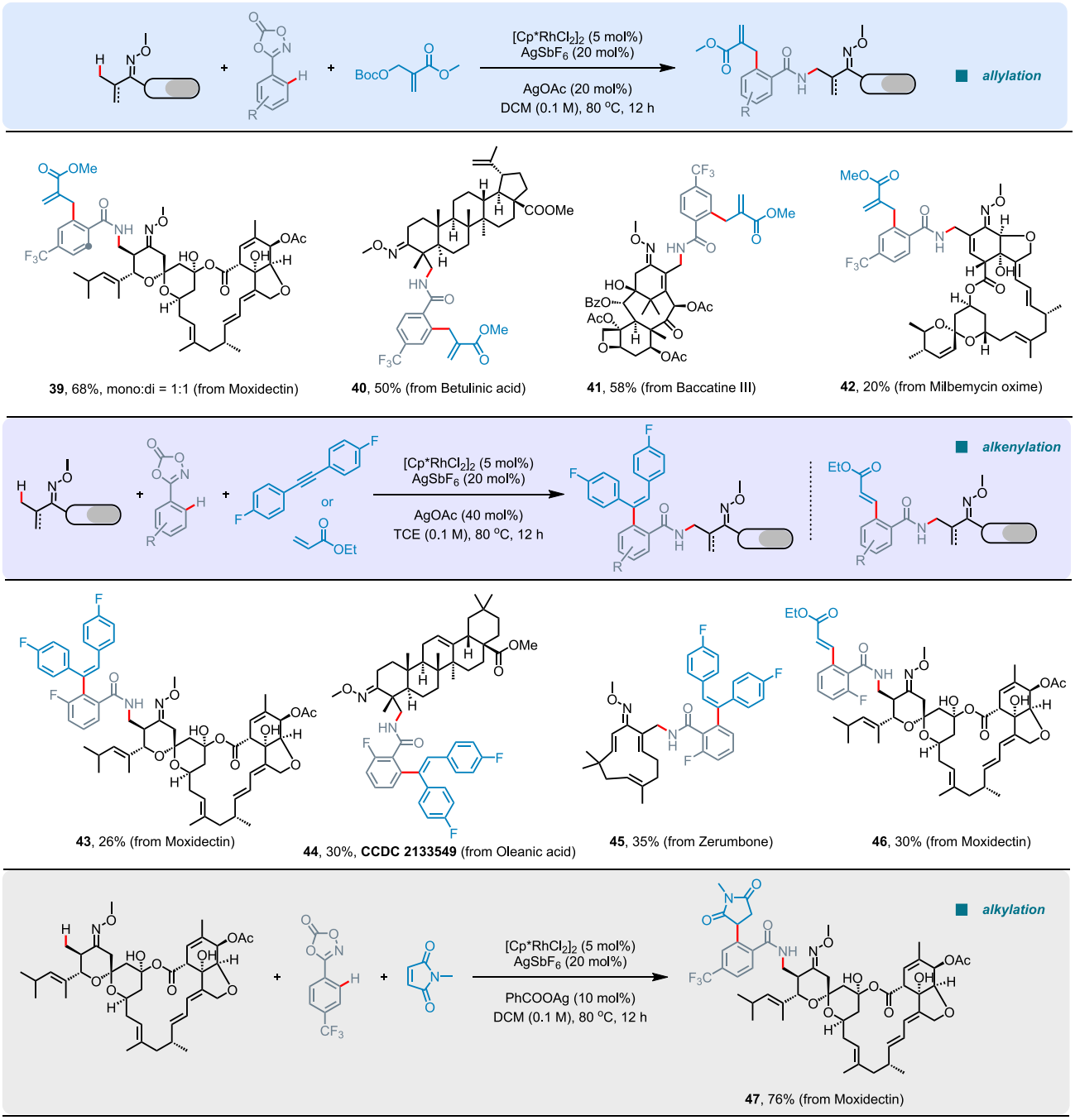

Figure 4. Late-stage diversification of complex molecules

Yields are based on a 0.1 mmol scale reaction after silica gel chromatography. Reaction conditions are not the same for different substrates. If reaction conditions for specific substrates were needed, please refer to the supplemental information.

products were generated via Rh-catalyzed C–H amidation/olefination macrocyclization. This differentiation is likely due to the distinct β-O and β-H elimination pathways.[53,54]

The preparation of complex macrocycles via the streamlined C–H functionalization of readily accessible, simple feedstocks, such as ketones, alcohols, and carboxylic

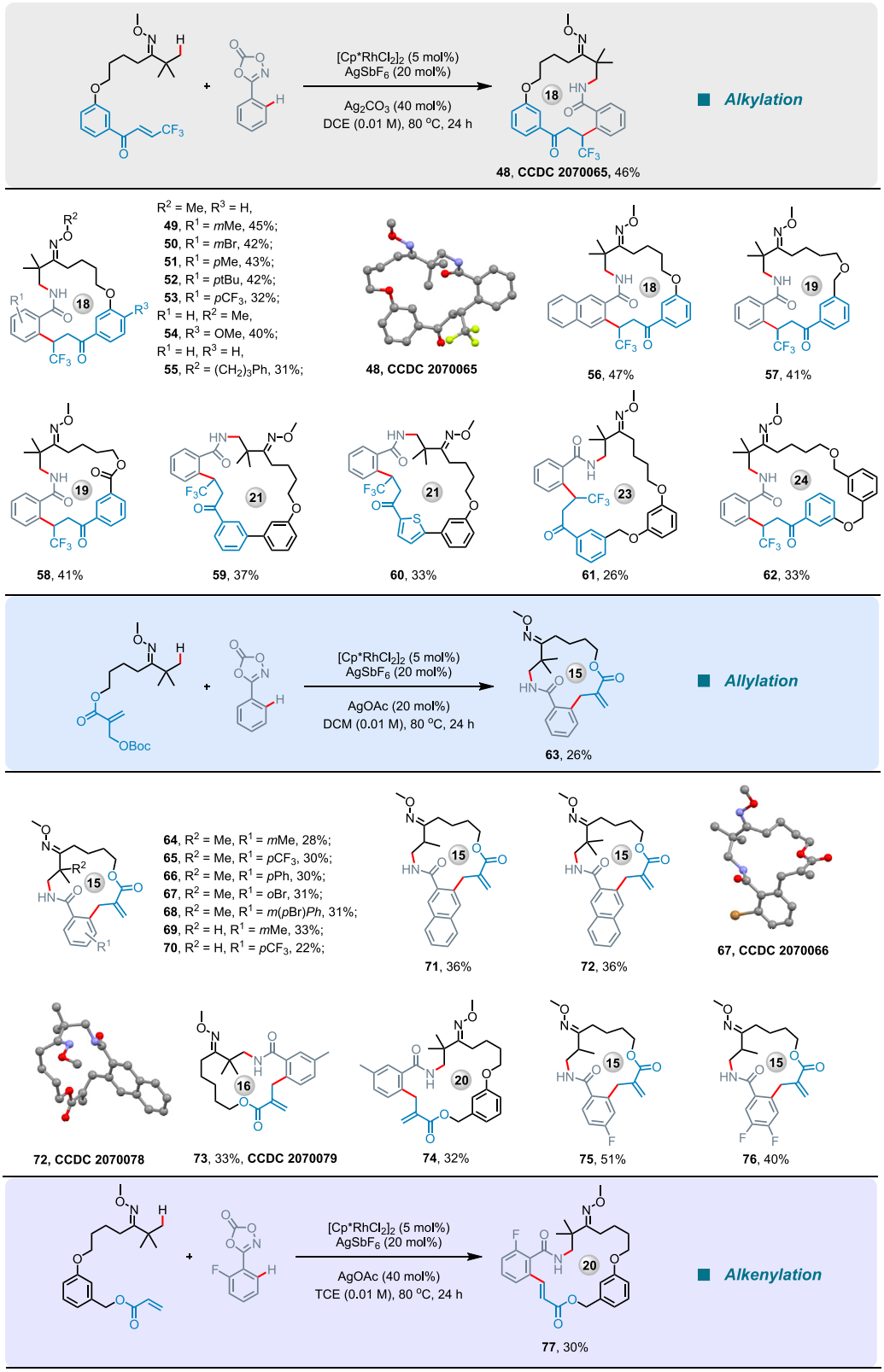

Figure 5. Scope of Rh(III)-catalyzed macrocyclization

Yields are based on a 0.1 mmol scale reaction after silica gel chromatography. Reaction conditions are not the same for different macrocyclizations. If reaction conditions for specific substrates were needed, please refer to the supplemental information.

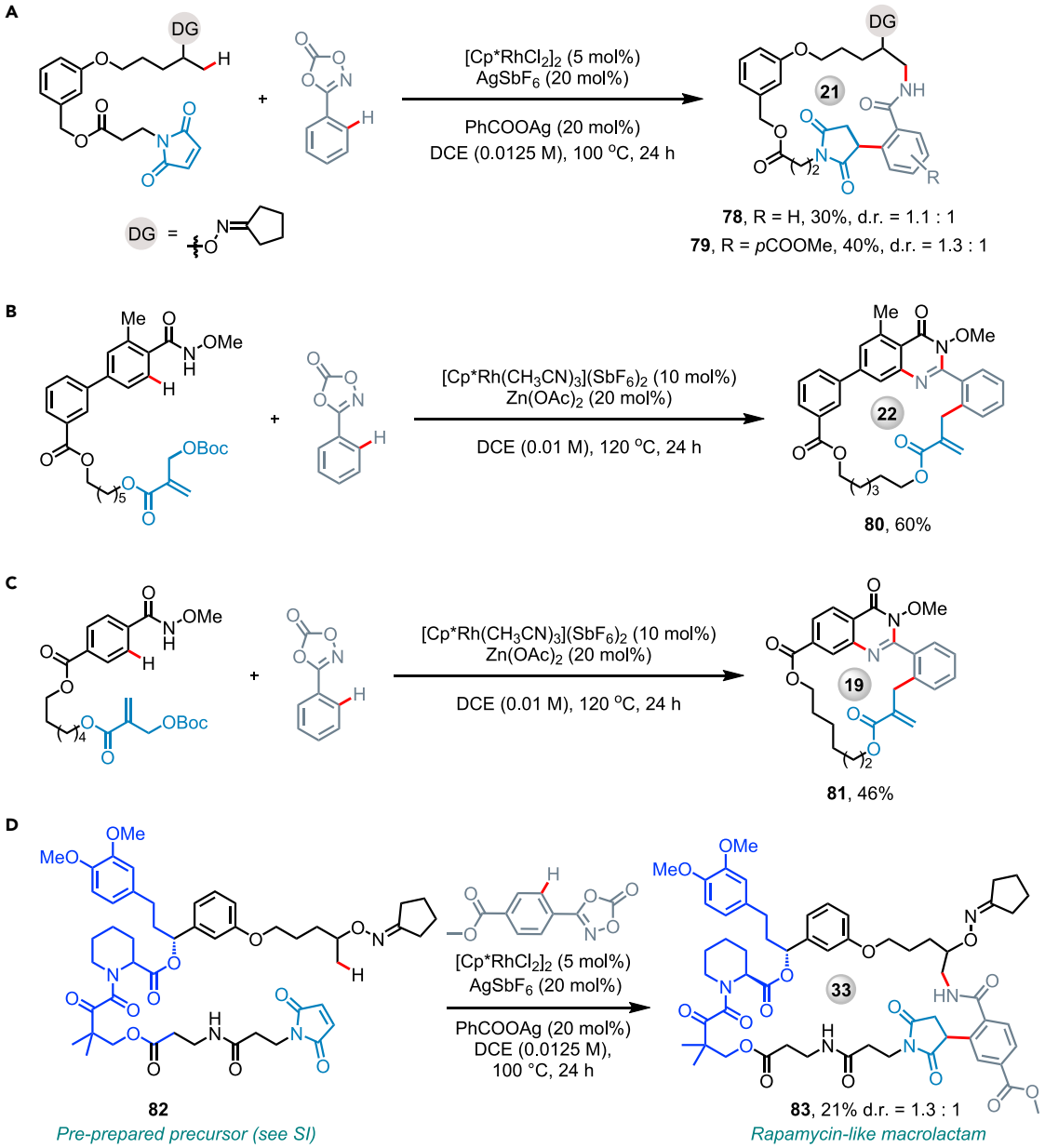

Figure 6. Further expanded scope of Rh(III)-catalyzed macrocyclization

Yields are based on a 0.1 mmol scale reaction after silica gel chromatography. Reaction conditions are not the same. If reaction conditions for specific substrates were needed, please refer to the supplemental information.

acids, is highly attractive to chemists. Given the success of the two-component dual C–H activation macrocyclization of ketone derivatives, we turned our attention to investigating the generality of our strategy by employing alcohol and carboxylic acid derivatives. As depicted in Figure 6, we found that these linear precursors can be smoothly macrocyclized using aryl-substituted 1,4,2-dioxazol-5-ones (**78–81**), highlighting the excellent compatibility of the developed *in situ*-generated directing group strategy. Furthermore, we demonstrated the robustness and practicality of the developed Rh-catalyzed intermolecular macrocyclizations by performing gram scale reactions without erosion of the yields.

Please cite this article in press as: Wang et al., Multicomponent coupling and macrocyclization enabled by Rh(III)-catalyzed dual C–H activation: Macrocyclic oxime inhibitor of influenza H1N1, Chem (2022), https://doi.org/10.1016/j.chempr.2022.10.019

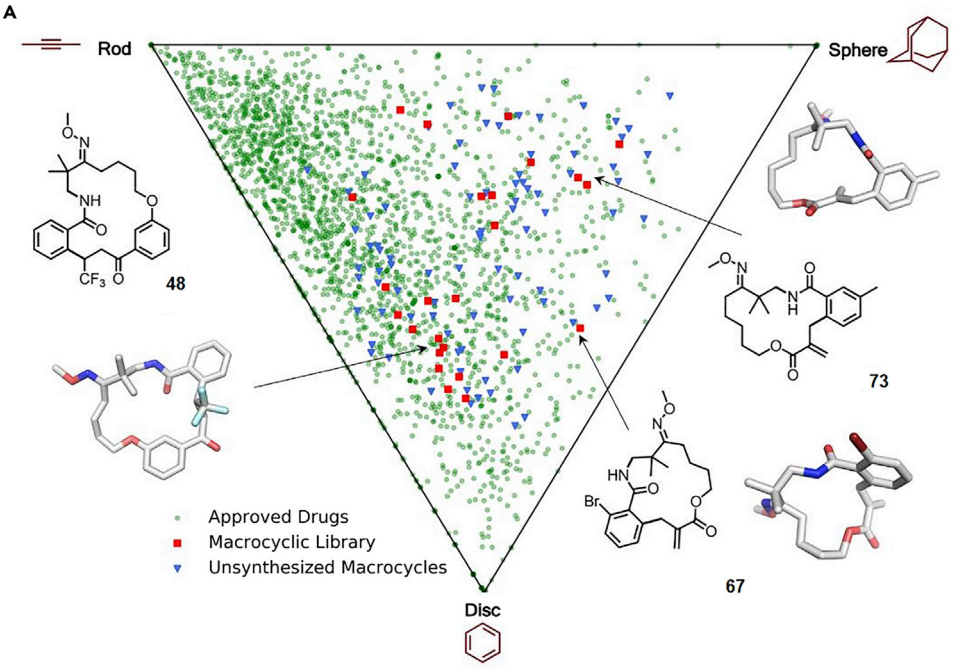

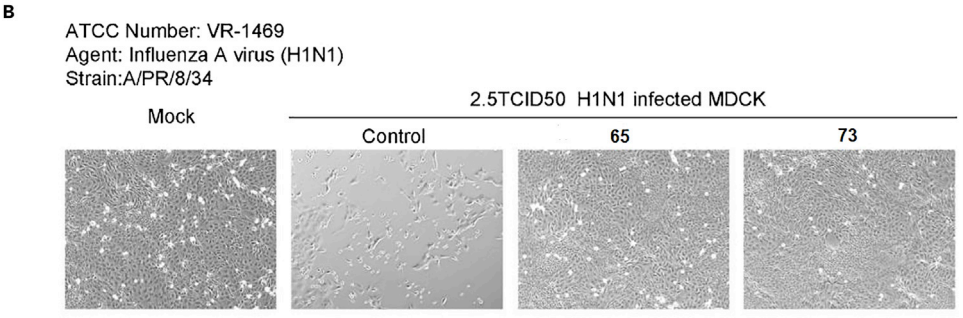

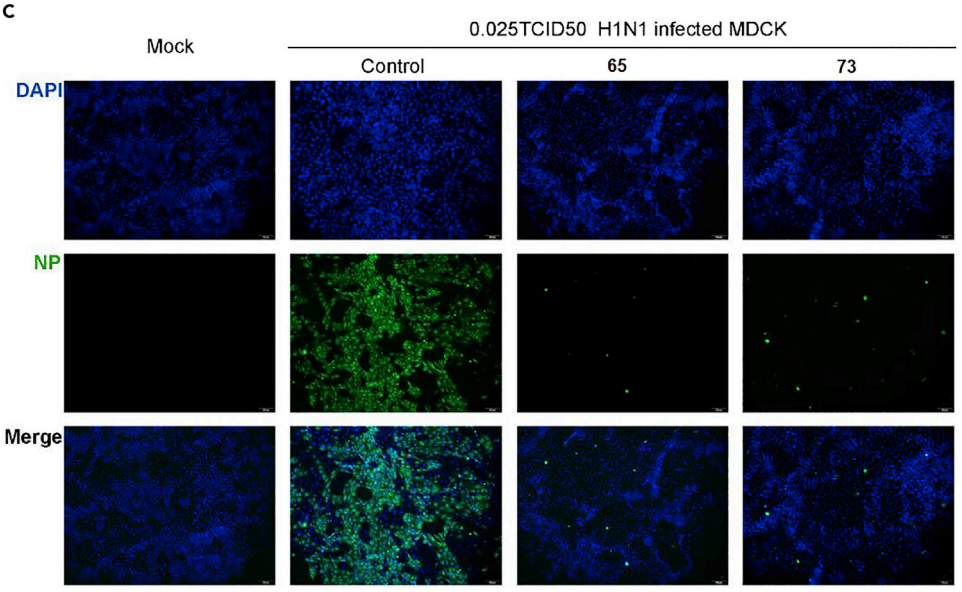

Figure 7. Principle moment-of-inactiveia plot and bioactivity studies

(A) The molecular shape diversity of the macrocyclic library (red squares), 87 unsynthesized macrocycles (filled blue triangles), and comparison with 2,402 approved drugs (open green dots). For further details, see supplemental information.

(B) The tested compounds ameliorated the cytopathic effects (cell rounding, degeneration, and sloughing) of H1N1 infection and improved cell survival.

(C) The compounds significantly decreased the signal for the nucleoprotein of H1N1. immunofluorescence, nucleoprotein (green); nucleus (4′,6-diamidino-2-phenylindole, DAPI, blue). See also Table S5 and Figure S4.

In addition, the identification of lead compounds greatly benefits from FBDD strategies. Therefore, to optimize lead compounds and highlight the potential application of this Rh-catalyzed two-component dual C–H activation macrocyclization in the construction of drug-like molecules, the privileged scaffold, FKBP-binding domain (FKBD) was initially extracted from Rapamycin.[55,56] Subsequently, this privileged scaffold was combined with suitably designed linkers to form a linear precursor (Figure 6E). Finally, an expedient synthesis of its analog was realized employing the developed protocol (**83**).

To assess the degree of the overall structural diversity attained in our macrocyclic library, we compared our set of macrocycles with approved drugs: (1) a set of 25 macrocycles from the synthesized library, (2) a set of 87 unsynthesized macrocycles potentially accessible through the current method, and (3) a set of 2,402 known drugs. Based on our calculations of the lowest energy conformations of all the depicted molecules, normalized ratios of principal moment-of-inactiveia (PMI) molecular shape descriptors were plotted on two-dimensional triangular graphs and then used to compare the structural space covered by different compound sets to rapidly assess and visualize the diversity in the molecular structures associated with a given compound set.[57,58]

As shown in the PMI plot (Figure 7A; see also Figure S5), all of the molecules were classified as rods, discs, or spheres to characterize the shape and distribution of the library around the triangle, which demonstrated the molecular structural diversity of the compound library. This figure shows that the vast majority of approved small molecule drugs are either rodlike or disklike,[59,60] whereas the current macrocyclic library discretely populates the third dimension in structural space, suggesting that it contains a considerably higher number of scaffold types and spherical molecules that are rare in conventional compound libraries, highlighting the advantage of this modular synthetic method in terms of product diversity.

Applying the above method, we created a screening library of various macrocycles. The benzamide-embedded oxime-substituted products were further investigated in various phenotypic assays to evaluate their influence on various biological processes; anti-inflammatory and anti-tumor effects and inhibitory activity against influenza A viruses were evaluated. Interestingly, the quantitative real-time PCR and cytopathic effect (CPE) inhibition assay revealed that several members of the collection inhibited the multiplication of H1N1 (strain: A/PR/8/34) and significantly increased cell survival after viral infection.

The SAR analysis of these novel macrocycles is presented in Table 1. Surprisingly, the CF_3-substituted macrocycles obtained via the cascade C–H amidation/alkylation route displayed minimal inhibitory activity against the multiplication of H1N1. However, the incorporation of α, β-unsaturated esters into the macrocycles through cascade C–H amidation/allylation significantly increased the inhibitory potency in most cases—the α, β-unsaturated ester as a Michael acceptor is known to be an irreversible inhibitor in drug discovery. Arylamides bearing electron-withdrawing groups (R^4) exhibited better potency than arylamides containing electron-donating groups in 15-membered

Please cite this article in press as: Wang et al., Multicomponent coupling and macrocyclization enabled by Rh(III)-catalyzed dual C–H activation: Macrocyclic oxime inhibitor of influenza H1N1, Chem (2022), https://doi.org/10.1016/j.chempr.2022.10.019

Table 1. Inhibitory activities of benzamide-embedded oxime-substituted macrocycles against influenza A H1N1 and structure-activity relationship analysis

48	49	50	51	52	53	54	55	56
57	58	59	60	61	62	63	64	65
65-1	65-2	66	67	68	69	70	71	72
73	74	75	76	77	78	79	80	81

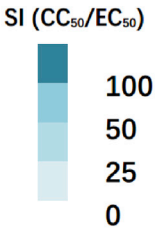

Entry	Compound	CC_{50} (μM)	EC_{50} (μM)	SI (CC_{50}/EC_{50})
1	48	26.29	NA	–
2	52	>100	NA	–
3	53	>100	NA	–
4	55	45.61	NA	–
5	56	100	NA	–
6	61	45.61	36.65	1.24
7	63	>100	NA	–
8	65	210.6	2.30	91.57
9	65-1	>100	NA	–
10	65-2	>100	NA	–
11	66	>100	NA	–
12	69	>100	9.84	>10.17
13	70	>100	0.57	>176.1
14	71	>100	2.15	>46.43
15	73	44.0	4.42	9.95
16	75	>100	1.78	56.27
17	76	>100	NA	–
18	77	>100	NA	–

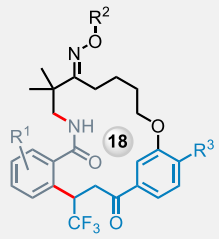

48 to **62**

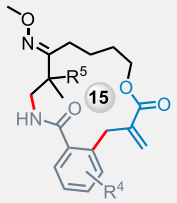

63 to **72**, **75** and **76**

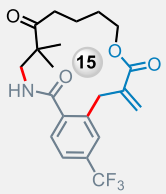

65-1

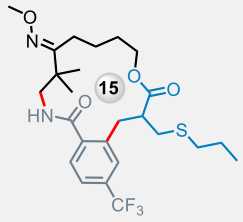

65-2

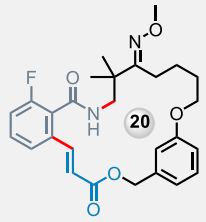

77

See also Table S6.

oxime-substituted macrocycles (**65** versus **66**). Removal of the oxime or masking the Michael acceptor as a thioether in macrocycle **65** produced macrocyclic ketone **65-1** and oxime **65-2**, respectively, which completely shut down the inhibitory activity. These results suggested that the oxime group and α, β-unsaturated ester were crucial macrocyclic components required for retaining the activity against influenza A and should be further investigated in drug design strategies against H1N1 infection. Remarkably, replacement of the R^5 methyl group of **65** with a hydrogen afforded **70**, which displayed enhanced potency with an IC_{50} value of 0.57 μM with an SI (selection index) value of >176. Based on the SAR analysis, representative compounds **65** and **73** were chosen for the CPE inhibition assay and immunofluorescence studies (Figures 7B and 7C; see also Table S5; Figures S3 and S4).[61] The signal strength for the nucleoprotein of infected Madin-Daby canine kidney (MDCK) cells decreased significantly after treatment with these compounds.

Please cite this article in press as: Wang et al., Multicomponent coupling and macrocyclization enabled by Rh(III)-catalyzed dual C–H activation: Macrocyclic oxime inhibitor of influenza H1N1, Chem (2022), https://doi.org/10.1016/j.chempr.2022.10.019

Conclusions

We report an *in situ*-generated directing group strategy and a two-component dual C–H activation macrocyclization mode that enables modular, versatile, and potentially enantioselective construction of various macrocycles, which may be of interest in medicinal chemistry and materials science. Using the developed method, a small screening library was rapidly obtained and assessed for potency against the H1N1 virus, showing promising results. The synthesized molecules were more spherical in shape than previous examples of macrocyclic drugs, expanding the chemical space of such molecules and opening up the possibility of future exploration through this synthetic method.

EXPERIMENTAL PROCEDURES

Resource availability

Lead contact

Further information and requests for resources and reagents should be directed to and will be fulfilled by the lead contact, Weibo Yang (yweibo@simm.ac.cn).

Materials availability

This study did not generate new unique reagents.

Data and code availability

All original data reported in the paper is available in the paper's supplemental information.

General procedure for the Rh(III)-catalyzed three-component coupling

A screw-capped vial was charged with the respective oxime (0.2 mmol, 2.0 equiv), dioxazolone (0.1 mmol, 1.0 equiv), alkene or alkyne (0.15 mmol, 1.5 equiv), $[Cp^*RhCl_2]_2$ (5 mol %), $AgSbF_6$ (20 mol %) and AgOAc (20 mol %) in 1.0 mL solvent (DCM or DCE, 1.0 mL, see the supplemental information for more details) under an air atmosphere. The reaction mixture was mixed uniformly, then stirred at 80°C for 12 h. After that, the vial was cooled to r.t., quenched with saturated brine and extracted with DCM. The combined organic layers were dried over anhydrous Na_2SO_4, filtered and concentrated in vacuo to give the residue. The residue was purified by flash chromatography on silica gel to afford the corresponding target product.

General procedure for the Rh(III)-catalyzed macrocyclization

A teflon-capped vial was charged with the respective linear precursor (0.2 mmol, 2.0 equiv), dioxazolone (0.1 mmol, 1.0 equiv), $[Cp^*RhCl_2]_2$ (5 mol %), $AgSbF_6$ (20 mol %), and AgOAc (20 mol %) in 10 mL DCM under an air atmosphere. The reaction mixture was mixed uniformly, then stirred at 80°C for 24 h. After that, the vial was cooled to r.t, quenched with saturated brine, and extracted with DCM. The combined organic layers were dried over anhydrous Na_2SO_4, filtered, and concentrated *in vacuo* to give the residue. The residue was purified by flash chromatography on silica gel to afford the corresponding target macrolactam.

Full experimental procedures are provided in the supplemental information.

SUPPLEMENTAL INFORMATION

Supplemental information can be found online at https://doi.org/10.1016/j.chempr.2022.10.019.

ACKNOWLEDGMENTS

We gratefully acknowledge 100 talent program of Chinese Academy of Sciences, "1000-Youth Talents Plan," NSFC (22171275), Shanghai-Youth Talent, National Science & Technology Major Project"Key New Drug Creation and Manufacturing Program" China (number: 2018ZX09711002-006), Science and Technology Commission of Shanghai Municipality (18431907100), Shanghai-Technology Innovation Action Plan (18JC1415300), and the National Science Foundation under the CCI Center for Selective C–H Functionalization (CHE-1700982), for financial support of this research.

AUTHOR CONTRIBUTIONS

W.Y. conceived the project and wrote the paper. K.H. supervised the DFT study. H.W., Z.L., T.B, X.T., Z.X., M.Z., Y.W., L.T., B.L., X.Z., and D.X., performed the experiments. X.C. and J.J.W. performed the DFT calculation. L.Y. performed the biologic studies. W.H. and J.Z. discussed the results and commented on the manuscript.

DECLARATION OF INTERESTS

The authors declare no competing interests.

INCLUSION AND DIVERSITY

We support inclusive, diverse, and equitable conduct of research.

Received: June 9, 2022
Revised: August 26, 2022
Accepted: October 18, 2022
Published: November 10, 2022

REFERENCES

1. Driggers, E.M., Hale, S.P., Lee, J., and Terrett, N.K. (2008). The exploration of macrocycles for drug discovery—an underexploited structural class. Nat. Rev. Drug Discov. *7*, 608–624.
2. Hamley, I.W. (2014). Peptide nanotubes. Angew. Chem. Int. Ed. Engl. *53*, 6866–6881.
3. Cummings, M.D., and Sekharan, S. (2019). Structure-based macrocycle design in small-molecule drug discovery and simple metrics to identify opportunities for macrocyclization of small-molecule ligands. J. Med. Chem. *62*, 6843–6853.
4. Dougherty, P.G., Qian, Z., and Pei, D. (2017). Macrocycles as protein–protein interaction inhibitors. Biochem. J. *474*, 1109–1125.
5. Liu, Y., Zhao, W., Chen, C.H., and Flood, A.H. (2019). Chloride capture using a C–H hydrogen-bonding cage. Science *365*, 159–161.
6. Nielsen, T.E., and Schreiber, S.L. (2008). Towards the optimal screening collection: a synthesis strategy. Angew. Chem. Int. Ed. Engl. *47*, 48–56.
7. Luo, T., and Schreiber, S.L. (2009). Gold(I)-catalyzed coupling reactions for the synthesis of diverse small molecules using the build/couple/pair strategy. J. Am. Chem. Soc. *131*, 5667–5674.
8. Beckmann, H.S.G., Nie, F., Hagerman, C.E., Johansson, H., Tan, Y.S., Wilcke, D., and Spring, D.R. (2013). A strategy for the diversity-oriented synthesis of macrocyclic scaffolds using multidimensional coupling. Nat. Chem. *5*, 861–867.
9. Grossmann, A., Bartlett, S., Janecek, M., Hodgkinson, J.T., and Spring, D.R. (2014). Diversity-oriented synthesis of drug-like macrocyclic scaffolds using an orthogonal organo- and metal catalysis strategy. Angew. Chem. Int. Ed. Engl. *53*, 13093–13097.
10. Isidro-Llobet, A., Hadje Georgiou, K., Galloway, W.R.J.D., Giacomini, E., Hansen, M.R., Méndez-Abt, G., Tan, Y.S., Carro, L., Sore, H.F., and Spring, D.R. (2015). A diversity-oriented synthesis strategy enabling the combinatorial-type variation of macrocyclic peptidomimetic scaffolds. Org. Biomol. Chem. *13*, 4570–4580.
11. Song, B., Xie, P., Li, Y., Hao, J., Wang, L., Chen, X., Xu, Z., Quan, H., Lou, L., Xia, Y., et al. (2020). Pd-catalyzed decarboxylative olefination: stereoselective synthesis of polysubstituted butadienes and macrocyclic P-glycoprotein inhibitors. J. Am. Chem. Soc. *142*, 9982–9992.
12. Chen, L., Quan, H., Xu, Z., Wang, H., Xia, Y., Lou, L., and Yang, W. (2020). A modular biomimetic strategy for the synthesis of macrolide P-glycoprotein inhibitors via Rh-catalyzed C–H activation. Nat. Commun. *11*, 2151.
13. Hao, J., Guo, X., He, S., Xu, Z., Chen, L., Li, Z., Song, B., Zuo, J., Lin, Z., and Yang, W. (2021). Marine furanocembranoids-inspired macrocycles enabled by Pd-catalyzed unactivated C(sp^3)-H olefination mediated by donor/donor carbenes. Nat. Commun. *12*, 1304.
14. Sun, T., He, S., Xu, Z., Zuo, J., Yu, Y., and Yang, W. (2021). Rh-catalyzed C–H alkylation enabling modular synthesis of CF_3-substituted benzannulated macrocyclic inhibitors of B cell responses. Org. Biomol. Chem. *19*, 3589–3594.
15. Yu, X., and Sun, D. (2013). Macrocyclic drugs and synthetic methodologies toward macrocycles. Molecules *18*, 6230–6268.
16. Mortensen, K.T., Osberger, T.J., King, T.A., Sore, H.F., and Spring, D.R. (2019). Strategies for the diversity-oriented synthesis of macrocycles. Chem. Rev. *119*, 10288–10317.
17. Saridakis, I., Kaiser, D., and Maulide, N. (2020). Unconventional macrocyclizations in natural product synthesis. ACS Cent. Sci. *6*, 1869–1889.
18. Ning, Y., Ohwada, T., and Chen, F.-E. (2021). Transition metal-catalyzed branch-selective hydroformylation of olefins in organic synthesis. Green Synth. Catal. *2*, 247–266.
19. Murray, C.W., and Rees, D.C. (2009). The rise of fragment-based drug discovery. Nat. Chem. *1*, 187–192.
20. Bissaro, M., Sturlese, M., and Moro, S. (2020). The rise of molecular simulations in fragment-based drug design (FBDD): an overview. Drug Discov. Today *25*, 1693–1701.

21. Erlanson, D.A., Fesik, S.W., Hubbard, R.E., Jahnke, W., and Jhoti, H. (2016). Twenty years on: the impact of fragments on drug discovery. Nat. Rev. Drug Discov. *15*, 605–619.

22. Jia, P., Pei, J., Wang, G., Pan, X., Zhu, Y., Wu, Y., and Ouyang, L. (2022). The roles of computer-aided drug synthesis in drug development. Green Synth. Catal. *3*, 11–24.

23. Boyd, M.R., and Paull, K.D. (1995). Some practical considerations and applications of the National Cancer Institute in vitro anticancer drug discovery screen. Drug Dev. Res. *34*, 91–109.

24. Weinstein, J.N., Myers, T.G., O'Connor, P.M., Friend, S.H., Fornace, A.J., Kohn, K.W., Fojo, T., Bates, S.E., Rubinstein, L.V., Anderson, N.L., et al. (1997). An information-intensive approach to the molecular pharmacology of cancer. Science *275*, 343–349.

25. Bulgaru, C.V., Marin, D.E., Pistol, G.C., and Taranu, I. (2021). Zearalenone and the immune response. Toxins *13*, 248.

26. Bryskier, A. (1998). Roxithromycin: review of its antimicrobial activity. J. Antimicrob. Chemother. *41*, 1–21.

27. Rivera, D.G., Ojeda-Carralero, G.M., Reguera, L., and Van der Eycken, E.V. (2020). Peptide macrocyclization by transition metal catalysis. Chem. Soc. Rev. *49*, 2039–2059.

28. SenGupta, S., and Mehta, G. (2020). Macrocyclization via C–H functionalization: a new paradigm in macrocycle synthesis. Org. Biomol. Chem. *18*, 1851–1876.

29. Dong, H., Limberakis, C., Liras, S., Price, D., and James, K. (2012). Peptidic macrocyclization via palladium-catalyzed chemoselective indole C-2 arylation. Chem. Commun. (Camb) *48*, 11644–11646.

30. Mendive-Tapia, L., Preciado, S., Garc´a, J., Ramón, R., Kielland, N., Albericio, F., and Lavilla, R. (2015). New peptide architectures through C–H activation stapling between tryptophan–phenylalanine/tyrosine residues. Nat. Commun. *6*, 7160.

31. Zhang, X., Lu, G., Sun, M., Mahankali, M., Ma, Y., Zhang, M., Hua, W., Hu, Y., Wang, Q., Chen, J., et al. (2018). A general strategy for synthesis of cyclophane-braced peptide macrocycles via palladium-catalysed intramolecular sp^3 C–H arylation. Nat. Chem. *10*, 540–548.

32. Bai, Z., Cai, C., Yu, Z., and Wang, H. (2018). Backbone-enabled directional peptide macrocyclization through late-stage palladium-catalyzed δ-C(sp 2)–H Olefination. Angew. Chem. Int. Ed. *57*, 13912–13916.

33. Ruan, Z., Sauermann, N., Manoni, E., and Ackermann, L. (2017). Manganese-catalyzed C–H alkynylation: expedient peptide synthesis and modification. Angew. Chem. Int. Ed. Engl. *56*, 3172–3176.

34. Wang, H., Tang, G., and Li, X. (2015). Rhodium(III)-catalyzed amidation of unactivated C(sp^3)-H bonds. Angew. Chem. Int. Ed. *54*, 13049–13052.

35. Tan, P.W., Mak, A.M., Sullivan, M.B., Dixon, D.J., and Seayad, J. (2017). Thioamide-directed cobalt(III)-catalyzed selective amidation of C(sp^3)–H bonds. Angew. Chem. Int. Ed. Engl. *56*, 16550–16554.

36. Shi, H., and Dixon, D.J. (2019). Dithiane-directed Rh(iii)-catalyzed amidation of unactivated C(sp^3)–H bonds. Chem. Sci. *10*, 3733–3737.

37. Hong, S.Y., Park, Y., Hwang, Y., Kim, Y.B., Baik, M.H., and Chang, S. (2018). Selective formation of γ-lactams via C–H amidation enabled by tailored iridium catalysts. Science *359*, 1016–1021.

38. Hwang, Y., Park, Y., Kim, Y.B., Kim, D., and Chang, S. (2018). Revisiting Arene C(sp^2)–H amidation by intramolecular transfer of iridium nitrenoids: evidence for a spirocyclization pathway. Angew. Chem. Int. Ed. Engl. *57*, 13565–13569.

39. Wang, H., Park, Y., Bai, Z., Chang, S., He, G., and Chen, G. (2019). Iridium-catalyzed enantioselective C(sp^3)–H amidation controlled by attractive noncovalent interactions. J. Am. Chem. Soc. *141*, 7194–7201.

40. Park, Y., and Chang, S. (2019). Asymmetric formation of γ-lactams via C–H amidation enabled by chiral hydrogen-bond-donor catalysts. Nat. Catal. *2*, 219–227.

41. van Vliet, K.M., and de Bruin, B. (2020). Dioxazolones: stable substrates for the catalytic transfer of acyl nitrenes. ACS Catal. *10*, 4751–4769.

42. Wang, H., Jung, H., Song, F., Zhu, S., Bai, Z., Chen, D., He, G., Chang, S., and Chen, G. (2021). Nitrene-mediated intermolecular N–N coupling for efficient synthesis of hydrazides. Nat. Chem. *13*, 378–385.

43. Hong, S.Y., Hwang, Y., Lee, M., and Chang, S. (2021). Mechanism-guided development of transition-metal-catalyzed C–N bond-forming reactions using dioxazolones as the versatile amidating source. Acc. Chem. Res. *54*, 2683–2700.

44. Zhang, F.L., Hong, K., Li, T.J., Park, H., and Yu, J.Q. (2016). Organic chemistry. Functionalization of C(sp^3)-H bonds using a transient directing group. Science *351*, 252–256.

45. He, J., Wasa, M., Chan, K.S.L., Shao, Q., and Yu, J.Q. (2017). Palladium-catalyzed transformations of alkyl C–H bonds. Chem. Rev. *117*, 8754–8786.

46. He, C., Whitehurst, W.G., and Gaunt, M.J. (2019). Palladium-catalyzed C(sp^3)–H bond functionalization of aliphatic amines. Chem *5*, 1031–1058.

47. Liu, B., Romine, A.M., Rubel, C.Z., Engle, K.M., and Shi, B.F. (2021). Transition-metal-catalyzed, coordination-assisted functionalization of nonactivated C(sp^3)–H bonds. Chem. Rev. *121*, 14957–15074.

48. Maity, S., Potter, T.J., and Ellman, J.A. (2019). α-Branched amines by catalytic 1,1-addition of C–H bonds and aminating agents to terminal alkenes. Nat. Catal. *2*, 756–762.

49. Pinkert, T., Das, M., Schrader, M.L., and Glorius, F. (2021). Use of strain-release for the diastereoselective construction of quaternary carbon centers. J. Am. Chem. Soc. *143*, 7648–7654.

50. Zhou, Y., Wang, J., Gu, Z., Wang, S., Zhu, W., Aceña, J.L., Soloshonok, V.A., Izawa, K., and Liu, H. (2016). Next generation of fluorine-containing pharmaceuticals, compounds currently in phase II-III clinical trials of major pharmaceutical companies: new structural trends and therapeutic areas. Chem. Rev. *116*, 422–518.

51. Guillemard, L., Kaplaneris, N., Ackermann, L., and Johansson, M.J. (2021). Late-stage C–H functionalization offers new opportunities in drug discovery. Nat. Rev. Chem. *5*, 522–545.

52. Ben-Lulu, M., Gaster, E., Libman, A., and Pappo, D. (2020). Synthesis of biaryl-bridged cyclic peptides via catalytic oxidative cross-coupling reactions. Angew. Chem. Int. Ed. Engl. *59*, 4835–4839.

53. Song, G., Wang, F., and Li, X. (2012). C–C, C–O and C–N bond formation via rhodium(III)-catalyzed oxidative C–H activation. Chem. Soc. Rev. *41*, 3651–3678.

54. Wu, S., Huang, X., Wu, W., Li, P., Fu, C., and Ma, S. (2015). A C–H bond activation-based catalytic approach to tetrasubstituted chiral allenes. Nat. Commun. *6*, 7946.

55. Sun, L., Yan, Y., Lv, H., Li, J., Wang, Z., Wang, K., Wang, L., Li, Y., Jiang, H., and Zhang, Y. (2022). Rapamycin targets STAT3 and impacts c-Myc to suppress tumor growth. Cell Chem. Biol. *29*, 373–385.e6.

56. Guo, Z., Hong, S.Y., Wang, J., Rehan, S., Liu, W., Peng, H., Das, M., Li, W., Bhat, S., Peiffer, B., et al. (2019). Rapamycin-inspired macrocycles with new target specificity. Nat. Chem. *11*, 254–263.

57. Sauer, W.H.B., and Schwarz, M.K. (2003). Molecular shape diversity of combinatorial libraries: a prerequisite for broad bioactivity. J. Chem. Inf. Comput. Sci. *43*, 987–1003.

58. Karageorgis, G., Reckzeh, E.S., Ceballos, J., Schwalfenberg, M., Sievers, S., Ostermann, C., Pahl, A., Ziegler, S., and Waldmann, H. (2018). Chromopynones are pseudo natural product glucose uptake inhibitors targeting glucose transporters GLUT-1 and -3. Nat. Chem. *10*, 1103–1111.

59. Prosser, K.E., Stokes, R.W., and Cohen, S.M. (2020). Evaluation of 3-dimensionality in approved and experimental drug space. ACS Med. Chem. Lett. *11*, 1292–1298.

60. Yang, T., Li, Z., Chen, Y., Feng, D., Wang, G., Fu, Z., Ding, X., Tan, X., Zhao, J., Luo, X., et al. (2021). DrugSpaceX: a large screenable and synthetically tractable database extending drug space. Nucleic Acids Res. *49*, D1170–D1178.

61. Lee, C.C., Yang, C.Y., Lin, L.L., Ko, T.P., Chang, A.H.-L., Chang, S.S.-C., and Wang, A.H.J. (2019). An effective neutralizing antibody against influenza virus H1N1 from human B cells. Sci. Rep. *9*, 4546.